Article

Are *N*,*N*-Dihydrodiazatetracene Derivatives Antiaromatic?

Shaobin Miao, Scott M. Brombosz, Paul v. R. Schleyer, Judy I. Wu, Stephen Barlow, Seth R. Marder, Kenneth I. Hardcastle, and Uwe H. F. Bunz

J. Am. Chem. Soc., **2008**, 130 (23), 7339-7344 • DOI: 10.1021/ja077614p • Publication Date (Web): 14 May 2008

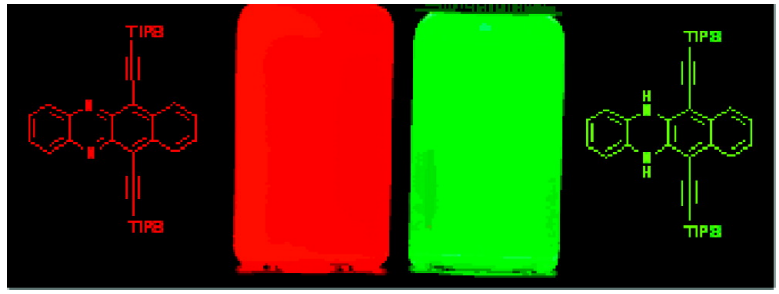

J|A|C|S
ARTICLES

Published on Web 05/14/2008

Are *N,N*-Dihydrodiazatetracene Derivatives Antiaromatic?

Shaobin Miao,[†] Scott M. Brombosz,[†] Paul v. R. Schleyer,[‡] Judy I. Wu,[‡] Stephen Barlow,[†] Seth R. Marder,[†] Kenneth I. Hardcastle,[§] and Uwe H. F. Bunz*,[†]

School of Chemistry and Biochemistry and Center for Organic Photonics and Electronics, Georgia Institute of Technology, Atlanta, Georgia 30332-0400, Department of Chemistry, University of Georgia, Athens, Georgia 30602-2556, and Department of Chemistry, Emory University, 1515 Dickey Drive, Atlanta, Georgia 30322

Received October 3, 2007; E-mail: uwe.bunz@chemistry.gatech.edu

Abstract: The synthesis and X-ray characterization of two new dialkynylated diazatetracenes and the corresponding *N,N*-dihydrodiazatetracenes are reported. The dialkynylated heteroacenes are packed in a brick-wall motif that enforces significant overlap of their π-faces. Cyclic voltammetry indicates that the dehydrogenated forms are easily reduced to their radical anions in solution. The planarity of these species validates the discussion of their aromaticity. Nucleus Independent Chemical Shift (NICS) computations demonstrate that both of these 20 π and 24 π electron systems are aromatic. Both experimental and computational results suggest that the aromaticity of the dihydroheteroacenes is reduced.

Introduction

The higher acenes have been widely used in organic electronics, due to their high charge carrier mobilities.[1] Pentacene in particular has potential in applications as thin-film p-channel transistors.[2] Its crystal packing exhibits significant $\pi-\pi$ intermolecular overlap, which contributes to its high charge carrier mobility.[2,3] Anthony has demonstrated that pentacenes, hexacenes, and heptacenes with strategically placed, sterically demanding alkyne substituents are stable and can be easily processed.[3] Their crystal structures can be manipulated predictably by the choice of appropriate substituents to maximize $\pi-\pi$ stacking in the solid state.[4] We now explore the potential elaboration of these systems by synthesizing and studying the properties of a pair of soluble, redox-related diaza- and dihydrodiazatetracenes.

The considerable interest in pentacene (~2000 papers, Web of Science) has only recently been extended to the larger nitrogen-containing heteroacenes, even though these have been known since the late 19th century.[5] Houk,[6] Wudl,[7] Nuckolls,[8] Tadokoro,[9] Jenekhe,[10] and Yamashita[11] have rejuvenated the field as large heteroacenes show potential as electron-transport materials.

Scheme 1. Interconversion of an Aromatic 6-π-Pyrazine Module into an Antiaromatic 8-π-Dihydropyrazine Module

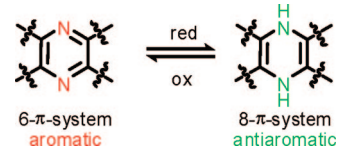

An underappreciated and rarely discussed aspect of the chemistry of the larger diazaacenes is their potential to be reduced (hydrogenated) to their formally antiaromatic congeners (Scheme 1, 2). Indeed, the dihydro forms of the diaza- and tetraazapentacenes seem to be remarkably viable.[5] Hinsberg reported that both the parent and the dihydro forms of diaza- and tetraazatetracenes appeared to be persistent, and he contended that the dihydro forms of the larger azaacenes were even more stable.[12] The notions of aromaticity and particularly of antiaromaticity[13] had not yet been developed in 1901. Consequently, the behavior of the formally antiaromatic dihydronaphthophenazine did not seem surprising at the time. This contri-

[†] Georgia Institute of Technology.
[‡] University of Georgia.
[§] Emory University.

(1) Nelson, S. F.; Lin, Y. Y.; Gundlach, D. J.; Jackson, T. N. *Appl. Phys. Lett.* **1998**, *72*, 1854–1856.
(2) (a) Dimitrakopoulos, C. D.; Malenfant, P. R. L. *Adv. Mater.* **2002**, *14*, 99–117. (b) Dimitrakopoulos, C. D.; Mascaro, D. J. *IBM J. Res. Develpment* **2001**, *45*, 11–27. (c) Reese, C.; Bao, Z. N. *J. Mater. Chem.* **2006**, *16*, 329–333. (d) Roberson, L. B.; Kowalik, J.; Tolbert, L. M.; Kloc, C.; Zeis, R.; Chi, X. L.; Fleming, R.; Wilkins, C. *J. Am. Chem. Soc.* **2005**, *127*, 3069–3075.
(3) (a) Anthony, J. E. *Chem. Rev.* **2006**, *106*, 5028–5048. (b) Anthony, J. E.; Brooks, J. S.; Eaton, D. L.; Parkin, S. R. *J. Am. Chem. Soc.* **2001**, *123*, 9482–9483. (c) Payne, M. M.; Parkin, S. R.; Anthony, J. E. *J. Am. Chem. Soc.* **2005**, *127*, 8028–8029. (d) Payne, M. M.; Delcamp, J. H.; Parkin, S. R.; Anthony, J. E. *Org. Lett.* **2004**, *6*, 1609–1612.
(4) Anthony, J. E.; Eaton, D. L.; Parkin, S. R. *Org. Lett.* **2002**, *4*, 15–18.
(5) (a) Fischer, O.; Hepp, E. *Chem. Ber.* **1890**, *23*, 2789–2798. (b) Fischer, O.; Hepp, E. *Chem. Ber.* **1900**, *33*, 1485–1498. (c) Kehrmann, F. *Chem. Ber.* **1890**, *23*, 2446–2454.
(6) Winkler, M.; Houk, K. N. *J. Am. Chem. Soc.* **2007**, *129*, 1805–1815.
(7) Wudl, F.; Koutenis, P. A.; Weitz, A.; Ma, B.; Strassner, T.; Houk, K. N.; Khan, S. I. *Pure Appl. Chem.* **1999**, *71*, 295–302.
(8) Miao, Q.; Nguyen, T. Q.; Someya, T.; Blanchet, G. B.; Nuckolls, C. *J. Am. Chem. Soc.* **2003**, *125*, 10284–10287.
(9) Tadokoro, M.; Yasuzuka, S.; Nakamura, M.; Shinoda, T.; Tatenuma, T.; Mitsumi, M.; Ozawa, Y.; Toriumi, K.; Yoshino, H.; Shiomi, D.; Sato, K.; Takui, T.; Mori, T.; Murata, K. *Angew. Chem., Int. Ed.* **2006**, *45*, 5144–5147.
(10) Jenekhe, S. A. *Macromolecules* **1991**, *24*, 1–10.
(11) Nishida, J.; Naraso; Murai, S.; Fujiwara, E.; Tada, H.; Tomura, M.; Yamashita, Y. *Org. Lett.* **2004**, *6*, 2007–2010.
(12) Hinsberg, O. *Liebigs Ann. Chem.* **1901**, *319*, 257–286.
(13) Breslow, R.; Brown, J.; Gajewski, J. J. *J. Am. Chem. Soc.* **1967**, *89*, 4383–4390.

Scheme 2. Synthesis of the Heteroacene **5a,b** and Dihydroheteroacene **6a,b**[a]

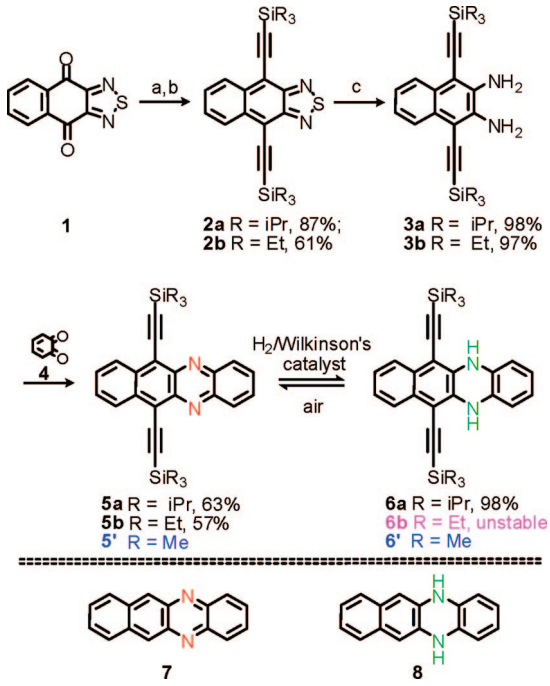

[a] (a) R_3Si-CC-Li, then wet ether; **a** R = isopropyl, **b** R = ethyl; (b) KI, NaH_2PO_2, AcOH; (c) $LiAlH_4$, THF.

bution illuminates the stabilities and spectroscopic properties of **5**−**8** in relationship to their aromatic/antiaromatic character.

Results and Discussion

Synthesis. The addition of the lithium salt of (triisopropylsilyl)acetylene or (triethylsilyl)acetylene to quinone **1**[14] generates an intermediate diol which reacts with potassium iodide and sodium hypophosphite in acetic acid into the naphthothiadiazole derivatives **2a,b**.[15] $LiAlH_4$ reduction of **2a,b** in THF afforded diamine **3a,b** in close to quantitative yields as blue-fluorescent, almost colorless powders. *ortho*-Quinone (**4**), obtained by oxidation of catechol in dichloromethane by acidic aqueous dichromate, was coupled with **3a,b** to furnish **5a,b** after flash chromatography (hexanes/dichloromethane 1/1) as dark-red, air-stable, crystalline materials.

X-Ray Crystal Structures of 5a,b, 7, and 8. The packing of **5a,b**, **7**, and **8** is of interest, as it determines the existence of short $\pi-\pi$ intrastack interactions, which is a necessary, although not sufficient, prerequisite for their successful incorporation into thin-film transistors or other organic electronic devices.

Crystalline specimens of **5a**, **5b**, **7**, and **8** were subjected to X-ray crystal-structure analysis; **5a**, **5b**, and **7** are stable under the crystallization conditions (dichloromethane/hexanes for **5a**,**b** and DMSO for **7**). Initial attempts to crystallize **8** from DMSO under ambient conditions gave red single crystals that had a crystallographic cell identical to that of **7**. But when crystallized from DMF in a dry box under exclusion of air, **8** was found to produce yellow platelets. Table 1 shows details of the four X-ray crystal structures. The structure of **5b** is better resolved, as the TIPS groups in **5a** are disordered, resulting in a high *R*-value

Table 1. Crystallographic Parameters of **5a**, **6a**, **7**, and **8**

a (Å)	*b* (Å)	*c* (Å)	α (deg)	β (deg)	γ (deg)	space group	*Z*	*R* (%)
5a	7.40	13.89	18.43	112	95.6	90.5 $P\bar{1}$	2	15
5b	7.21	13.69	30.89	90	102	90 $C2/c$	4	8.8
7	7.07	8.44	18.52	90	95.2	90 $P2_1/c$	4	4.0
8	5.83	7.85	12.51	101	101	94 $P\bar{1}$	2	4.5
TC[a]	6.06	7.84	13.01	77.1	72.1	85.8 $P\bar{1}$	2	5.7

[a] TC = Tetracene, data from: Holmes, D.; Kumaraswamy, S.; Matzger, A. J.; Vollhardt, K. P. C. *Chem. Eur. J.***1999**, *5*, 3399−3412.

of 15%; however, the packing is clearly discernible. The parent compounds **7** and **8** are well-behaved, and the crystal structures could be refined to give low *R*-values. Table 1 displays cell parameters and *R*-values. While **5a** and **8** are triclinic, **5b** and **7** pack in a monoclinic cell. Figures 1–3 display the packing patterns of **5a** and **5b**. *Despite their quite different unit cells, the packing of **5a** and **5b** is similar*. The most significant difference is illustrated in Figure 2; **5a** is arranged in a tilted fashion, while **5b** forms a rectangular pattern. The most likely reason for the subtle difference in packing is the increased steric demand of the TIPS group in comparison to that of the triethylsilyl substituent. A subtle difference in the tilt angle of the molecules within one stack differentiates **5a** from **5b**. The best description of the overall packing is perhaps that of a tilted brick wall, i.e., heteroacenes **5a,b** pack in a 2-D stack (see Supporting Information) but with a significant short-axis offset, similar to the case of acceptor-substituted tetracene derivatives prepared by Anthony et al.[16] The short intrastack distance of two molecules of **5a**, 3.35 Å, equals the combined van der Waals radii of carbon. A virtually identical value, 3.33 Å, is found for **5b**, which suggests that both heteroacenes have a packing arrangement desirable for molecular electronics applications. The size of the substituents on the alkynes has, in this case, only a relatively small effect on the overall packing of the heteroacenes **5a** and **5b**.

The crystal packing of the two parent heteroacenes **7** (Figure 5) and **8** (Figure 6) differs from that of **5a,b** (Figures 1–3) and tetracene.[17] Both **7** and **8** are nearly planar, but the NH groups in **8** are slightly puckered and the structure is disordered with respect to the relative position of the dihydropyrazine ring in the molecule. As the CH and NH groups are of similar size and steric bulk, the molecules of **8** pack as if they possess an inversion center (Figure 4). The planarity of **8** is relevant to the discussion of the question of aromaticity and/or antiaromaticity (vide infra). As shown in Figure 5, **7** displays a herringbone packing, in which the intrastack distance is approximately 3.8 Å along the *b*-axis. In contrast, **8** exhibits a face-to-edge arrangement, in which the $\pi-\pi$ stacking is absent (see Figure 6). Both **7** and **8** have unfavorable packing for high charge carrier mobility, since they have only modest (**7**) or absent (**8**) intrastack $\pi-\pi$ interactions. However, the packing of **5a,b** (Figures 1–3) enforces the intrastack $\pi-\pi$ interactions due to the presence of the silylated alkyne substituents. We were unable to obtain an X-ray crystal structure for **6a**, since **6a** oxidized quickly to **5a**, even in the crystalline state.

Electronic Spectra and Electrochemistry of 5−8. While 6,11-bis(triisopropylsilylethynyl)benzo[*b*]phenazine (**5a**) is nonfluo-

(14) Cava, M. P.; Schlessinger, R. H. *Tetrahedron Lett.* **1964**, 3815–3817.
(15) Miao, S.; Smith, M. D.; Bunz, U. H. F. *Org. Lett.* **2006**, *8*, 757–760. (b) Miao, S.; Schleyer, P. v. R.; Wu, J. I.; Hardcastle, K. I.; Bunz, U. H. F. *Org. Lett.* **2007**, *9*, 1073–1076.
(16) (a) Odom, S. A.; Parkin, S. R.; Anthony, J. E. *Org. Lett.* **2003**, *5*, 4245–4248. (b) Anthony J. E. In *Functional Organic Materials*; Bunz, U. H. F., Müller, T. J. J., Eds.; Wiley-VCH: Weinheim, 2007; pp 511−545.
(17) Holmes, D.; Kumaraswamy, S.; Matzger, A. J.; Vollhardt, K. P. C. *Chem. Eur. J.* **1999**, *5*, 3399–3412.

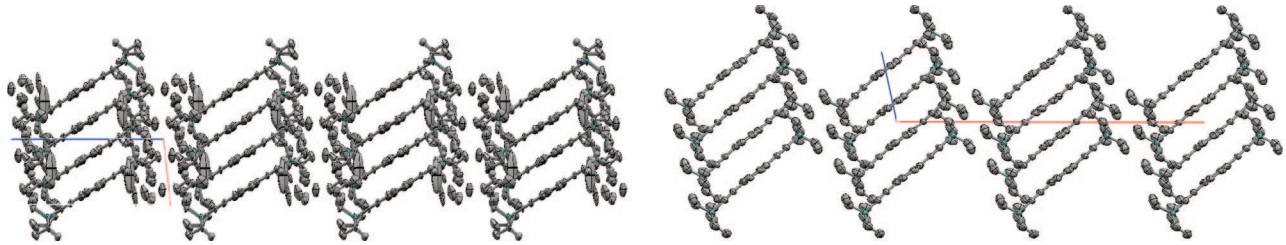

Figure 1. Packing of **5a** (left) and **5b** (right); view along the *b*-axis.

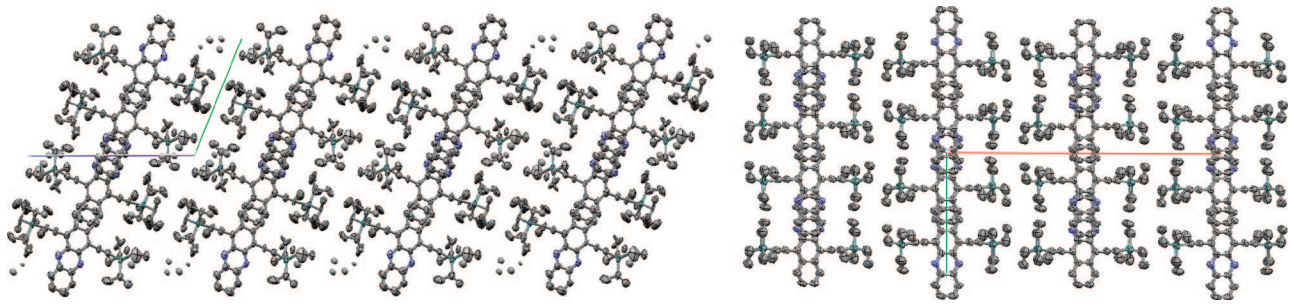

Figure 2. Packing of **5a** (left) and **5b** (right); view along the *a*-axis.

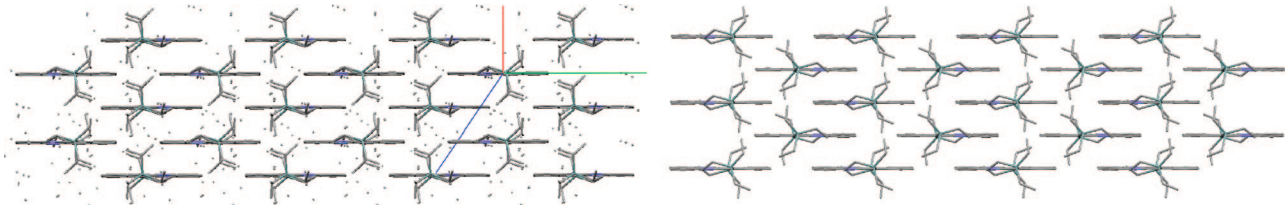

Figure 3. Stacking of **5a** (left) and **5b** (right), viewed along the axis that is formed by the two ethynyl substituents. Note that this view is *not* along any viable crystallographic main axis.

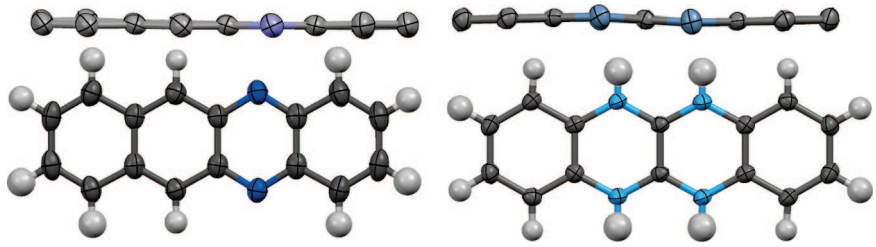

Figure 4. Molecular structures of **7** (left) and of **8** (right). The top view displays the planarity of both **7** and **8**. The four powder blue colored positions in **8** contain overall two nitrogen atoms in either the 5,12- or the 6,11-position as a consequence of the disorder of **8**, where it can take on two different orientations.

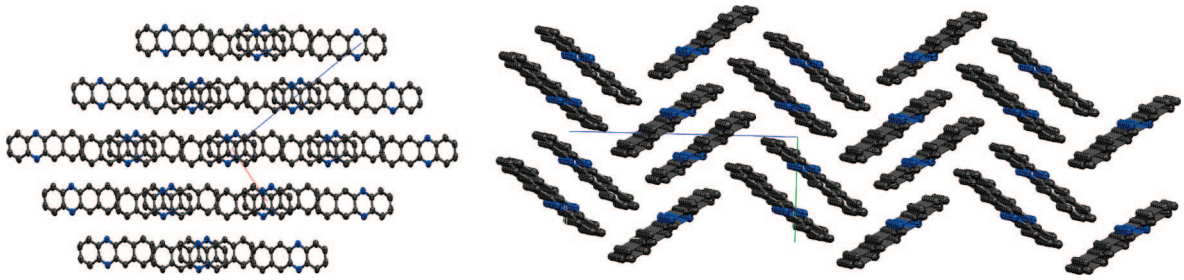

Figure 5. Packing of **7**. View along the *b*-axis (left) and along the *a*-axis (right).

rescent in the solid state, due to its intrastack interactions, it is red-fluorescent in solution with acene-type vibronic progressions in both absorption and emission (λ_{max} abs = 571 nm, λ_{max} emission = 583 nm, Figure 7);[18] **5a** is persistent and melts at 186 °C without decomposition. It can be hydrogenated at 2500 psi H_2 pressure using Wilkinson's catalyst ($(Ph_3P)_3RhCl$) to give a new, brightly yellow-green fluorescent compound (assigned

(18) Perkampus H.-H. *UV-Vis Atlas of Organic Compounds*, 2nd ed.; VCH: Weinheim, 1992.

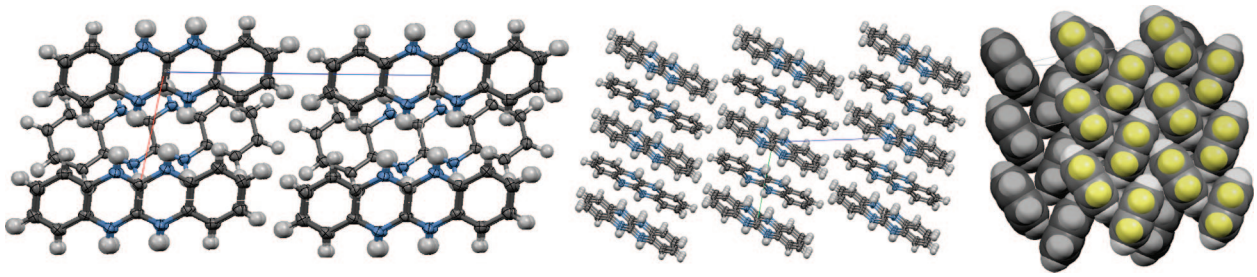

Figure 6. Packing of **8**. View along the *b*-axis (left) and along the *a*-axis (middle). View along the diagonal of the crystallographic *b*- and *c*-axes (right).

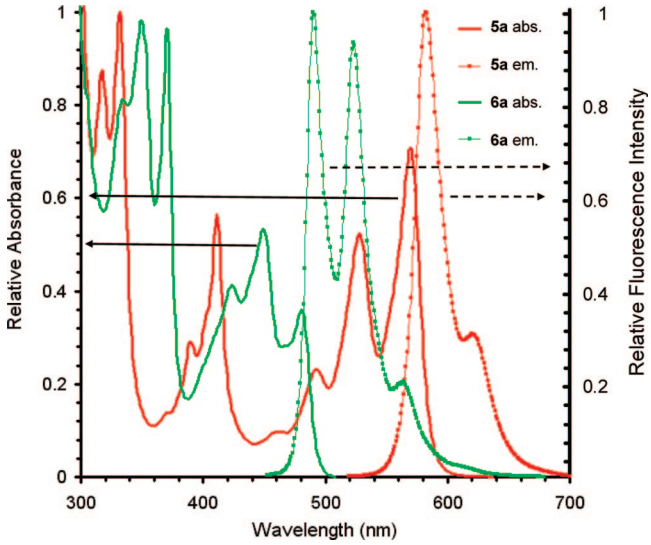

Figure 7. UV−vis and emission spectra of **5a** and **6a** in dichloromethane.

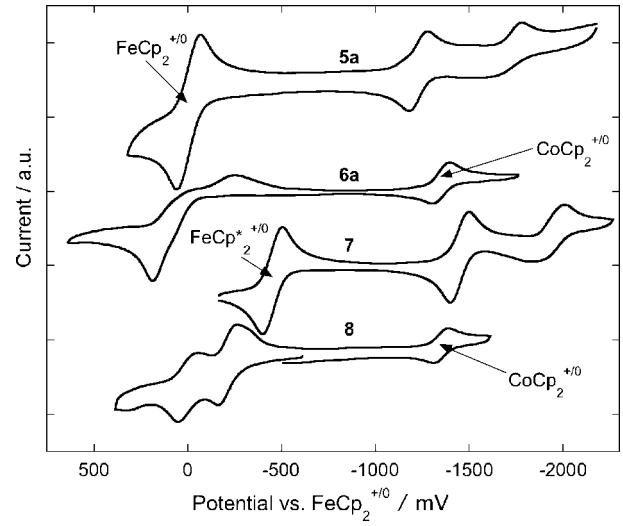

Figure 8. Cyclic voltammograms of **5a**, **6a**, **7**, and **8** in THF/0.1 M $^{n}Bu_4NPF_6$ recorded at 50 mV s^{-1}. Signals due to internal reference couples are indicated, different couples having been chosen for different compounds to avoid overlap. In all cases, the data have been plotted relative to the ferrocenium/ferrocene redox couple.

Table 2. Electrochemical Half-Wave Potentials (V vs Ferrocenium/Ferrocene) for **5a**, **6a**, **7**, and **8** in THF/0.1 M $^{n}Bu_4PF_6$

compd, M	$E_{1/2}(M^{2+/+})$ (V)	$E_{1/2}(M^{+/0})$ (V)	$E_{1/2}(M^{0/-})$ (V)	$E_{1/2}(M^{-/2-})$ (V)
5a	-	*a*	−1.23[a]	−1.78[a]
7	-	-	−1.44	−2.00[b]
6a	-	+0.19[b]	-	-
8	0.00	−0.21	-	-

[a] In CH_2Cl_2/0.1 M $^{n}Bu_4NPF_6$ a reversible oxidation is observed at +0.95 V; reversible and EC-type reductions are seen at −1.21 and −1.68 V, respectively, in the same solvent. [b] Irreversible, the given values correspond to the peak potentials of E_{red} (for **7**) and E_{ox} (for **6a**).

structure **6a**) in 98% yield. The absorption and emission spectra of **6a** are shown in Figure 7 (λ_{max} abs = 482 nm, λ_{max} emission = 491 nm). The NH units gave a distinct, sharp IR band at 3396 cm^{-1} and a single broad ^1H NMR peak. Otherwise, the NMR spectrum of **6a** is similar to that of **5a**, except that all the ^1H signals are shifted to higher field. Dihydroheteroacene **6a** is isolable but quickly reverts to **5a** on exposure to air, both in solution and in the solid state. The compound **6b** is so unstable that it oxidizes back to **5b** almost immediately. Interestingly, the acetylene substituents seem to decrease the persistence of **6a**, compared to Hinsberg's parent diazadihydrotetracene **8**.[12]

We performed cyclic voltammetry (CV) of **5a** and **6a** in THF/0.1 M $^{n}Bu_4NPF_6$ to examine their redox relationships in an electron-transfer rather than hydrogen-transfer sense. Sample voltammograms are shown in Figure 8, and their potentials are summarized in Table 2; **5a** undergoes a fully reversible first molecular reduction, at a similar potential as that for **7**. Both compounds also exhibit less chemically reversible reductions to the dianion at a more negative potential. For **7**, the second reduction is irreversible. The second reduction of **5a** shows the characteristics of an EC-type process, in which a reversible electron transfer is followed by chemical reaction on a comparable timescale. In CH_2Cl_2, **5a** also displays a reversible molecular oxidation at +0.95 V vs ferrocenium/ferrocene. The voltammograms of **6a** and **8** are different from one another: while the oxidation of **6a** is irreversible, **8** undergoes two successive more-or-less reversible oxidations.[19] The similarities between **5a** and **7** are obvious from the close values of their first and second reduction potentials as well as the reversibility of their electrochemistry. For **6a** and **8**, the origin of their differences in chemical reversibility is unknown, however, the irreversibility of $\mathbf{6a}^{+/0}$ may be related to its tendency to be oxidized (in the sense of hydrogen loss).

The electrochemical data also make possible a rough estimate of the solid-state ionization potentials and electron affinities, parameters important for potential applications in organic electronics. The solid-state electron affinity of **5a** can be

(19) (a) The overall process is chemically reversible; however, integration of the reduction wave for the $\mathbf{8}^{2+/+}$ process corresponds to less than one electron, while the $\mathbf{8}^{+/0}$ reduction wave corresponds to more than one electron. This may suggest coupled electron and proton transfer processes as have been seen for other phenazine derivatives; however, we have not investigated this aspect in detail. (b) Laviron, E.; Roullier, L. *J. Electroanal. Chem.* **1983**, *157*, 7–18. (c) Sawyer, D. T.; Komai, R. Y. *Anal. Chem.* **1972**, *44*, 715–721.

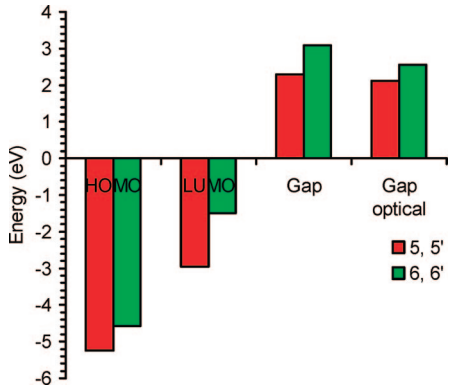

Figure 9. HOMO/LUMO energies and gap, computed at B3LYP/6-31G*// B3LYP/6-31G*, for **5′** (red) and **6′**(green), and optical data (Gap optical experimentally determined) for **5** and **6**.

estimated (as described in ref 20 and, in more detail, in the Supporting Information) as ca. −3.4 eV, approaching those estimated in the same way for well-established electron-transport materials with facile electron injection including perylene diimides (ca. −3.6 eV)[20a−c] and C_{60} (ca. −3.7 eV) and considerably more exothermic than that of Alq_3[20d] (ca. −2.3 eV), which is widely used as an electron-transport material in organic light-emitting diodes. The solid-state ionization potential of **5a** is estimated at ca. 6.1 eV (see Supporting Information), significantly higher than that of well-established hole-transport materials such as TIPS-pentacene (ca. 5.5 eV estimated by the same method from the potential given in ref 3d in the Supporting Information) and TPD (directly measured at 5.4 eV),[20e] suggesting a large barrier to hole injection from typical electrode materials used in organic electronics. The reversible reductions of **5a** and **7** reveal that the radical anions of these species are relatively stable. Moreover, their reduction potentials are in the vicinity of the solution reduction potential of molecular oxygen (for which we observe E_{red} at ca. −1.3 V vs $FeCp_2^{+/0}$ in THF/0.1 M $^nBu_4NPF_6$), suggesting the possibility of air-stable electron transport in these materials.

Computational Studies of the Aromaticity of 5−8. Despite the formally 4n π perimeter of **6a,b**, **6′**, and **8**, the computed heats of hydrogenation of **7** to **8** (ΔH_H = −20.8 kcal/mol at B3LYP/6-311+G** with ZPE correction) is only 5.8 kcal/mol more exothermic than that of the inner ring of tetracene (ΔH_H = −15.0 kcal/mol).

7 + H_2 → **8** ΔH_H = −20.8 kcal/mol

Tetracene + H_2 → 5,12-Dihydrotetracene ΔH_H = −15.0 kcal/mol

However, this comparison is influenced by the difference in CH vs NH bond energies. The computed heat of hydrogenation involving nonaromatic models, 2,3-dihydropyrazine and 1,2,3,4-tetrahydropyrazine (ΔH_H = −18.8 kcal/mol), is nearly the same as that of **7** to **8**. In contrast, the hydrogenation of 2,3-cyclohexadiene to cyclohexene (ΔH_H = −22.5 kcal/mol) is 7.5 kcal/mol more exothermic than that of tetracene to dihydrotetracene. Evidently, the loss of aromatic stabilization energy (ASE) upon the hydrogenation of **7** to **8** is less than that of tetracene to 5,12-dihydrotetracene, despite the 4n π perimeter of **8**.

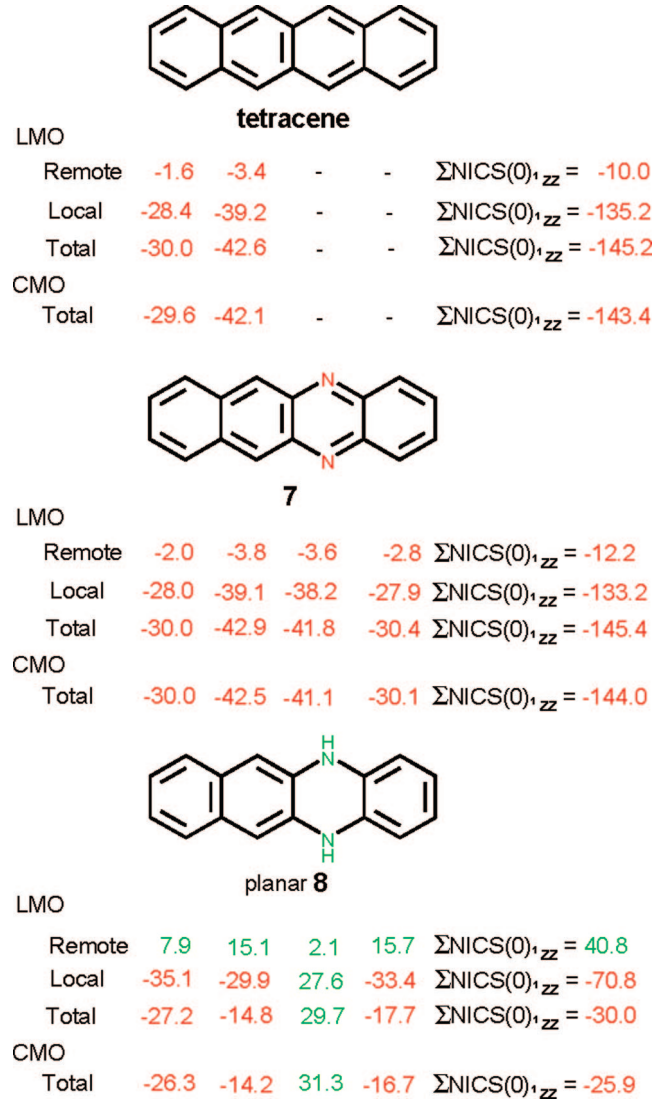

Figure 10. IGLO-LMO (localized molecular orbital) and GIAO-CMO (canonical molecular orbital) $NICS(0)_{\pi zz}$ computed at PW91/IGLO-III// B3LYP/6-311+G**. "Local" refers to the π LMO contributions of individual localized double bonds and lone pairs associated with the designated individual rings (when appropriate, localized exocyclic π bonds are included). "Remote" refers to the remaining π MO contributions. Note also that the sum of the remote and local total LMO contributions matches the CMO total closely. (The planar C_{2v} form of **8** had one imaginary frequency but has essentially the same energy as the C_s minimum.)

Diazatetracenes, like **5a,b** and **7**, certainly are aromatic, but are their 4n π dihydro derivatives really antiaromatic? NICS (nucleus independent chemical shift) computations at the centers of the individual rings of **7** and **8** (as well as tetracene for comparison) are revealing (Figure 10).[21] Our analysis employs the $NICS(0)_{\pi zz}$ index,[22] which is based on the out-of-plane tensor components of the canonical (CMO) or of localized (LMO) π molecular orbital contributions to the isotropic NICS. $NICS(0)_{\pi zz}$ data for both the dissected IGLO-LMO method (with Pipek−Mezey localization as implemented in the deMon

(20) (a) These estimates were made as previously described using Alq3 and TPD as references for EA and IP, respectively. As discussed, alternative less conservative (more exothermic) estimates of EA can be obtained using other comparisons. (b) Zhan, X.; Risko, C.; Amy, F.; Chan, C.; Zhao, W.; Barlow, S.; Kahn, A.; Brédas, J. L.; Marder, S. R. *J. Am. Chem. Soc.* **2005**, *127*, 9021–9029. (c) An, Z.; Yu, J.; Jones, S. C.; Barlow, S.; Yoo, S.; Domercq, B.; Prins, P.; Siebbeles, L. D. A.; Kippelen, B.; Marder, S. R. *Adv. Mater.* **2005**, *17*, 2580–2583. (d) Cahen, D.; Kahn, A. *Adv. Mater.* **2003**, *15*, 271–277. (e) Anderson, J. D.; McDonald, E. M.; Lee, P. A.; Anderson, M. L.; Ritchie, E. L.; Hall, H. K.; Hopkins, T.; Nash, E. A.; Wang, J.; Padias, A.; Thayumanavan, S.; Barlow, S.; Marder, S. R.; Jabbour, G.; Shaheen, S.; Kippelen, B.; Peyghambarian, N.; Wightman, R. M.; Armstrong, N. R. *J. Am. Chem. Soc.* **1998**, *120*, 9646–9655.

program)[23,24] and the GIAO-CMO[25] method are computed at PW91/IGLO-III//B3LYP/6-311+G** for uniformity.

As expected, all the individual local NICS(0)$_{\pi zz}$ values of **7** and the overall ΣNICS(0)$_{\pi zz}$ sums are highly diatropic and are similar to those of tetracene (Figure 10).[23] Both their total LMO and total CMO NICS(0)$_{\pi zz}$ data are almost identical. The LMO details are instructive. Note that the "local" and "total" LMO NICS(0)$_{\pi zz}$ data for both **7** and tetracene are very similar. Evidently, the large negative NICS(0)$_{\pi zz}$ values of the individual rings are due to their "local" diatropicity (i.e., the π contributions involving each ring itself). The "remote" π contributions (from the other rings) are rather small. In line with Clar's rule, which states that structures with a maximum number of localized sextet rings are advantageous energetically, the diatropic contributions of the aromatic subunits of both **7** and tetracene are localized. The inner rings of **7** and also more diatropic than the outer rings.[26]

The behavior of **8** is different. Both LMO and CMO ΣNICS(0)$_{\pi zz}$(−28 ± 2 ppm) reveal **8** to be *weakly aromatic* despite its 4n π perimeter (Figure 10). Note that the paratropic contributions of the dihydropyrazine ring of **8** are rather delocalized (see Figure 10). Unlike **7**, the "remote" LMO contributions of the individual aromatic rings of **8** (shown in green) are distinctly paratropic. For this reason, the ΣNICS(0)$_{\pi zz}$ of both tetracene and **7** (approximately −145 ppm) are much greater in magnitude than that of **8**. Note that the benzenoid rings of **8** have significantly less diatropic individual "total" LMO NICS(0)$_{\pi zz}$ values compared to their corresponding rings in **7**, but their "local" LMO NICS(0)$_{\pi zz}$ values are similar (see Figure 10). The "local" aromaticites of the bezenoid rings of **8** are preserved, despite the presence of the antiaromatic dihydro ring.

The magnetic criteria suggest that **8** and its derivatives **6a,b** are aromatic, even though less so than **7** and **5a,b**, at least when aromaticity is viewed as a *global* property. If one considers aromaticity as a local ring-by-ring rather than a global molecular property, **6** and **8** can be viewed as overall aromatic, yet the central dihydropyrazine ring in both is strongly (locally) antiaromatic, with an additional global component. However, upon dehydrogenation the strong local antiaromaticity disappears. On the other hand, part of the relative stability of **6** and **8** comes from the increased HOMO−LUMO gap (discussed below), another experimental and calculational observation that is at odds with both simple Hückel theory and the expectations fuelled by antiaromatic compounds such as cyclobutadiene. While **8** is easily isolated and characterized, **6a** and **6b** are less persistent, although **6b** is sufficiently stable to be characterized.

Moreover, the HOMO−LUMO gap of *aromatic* **5a,b** is smaller than that of the *formally antiaromatic* **6a,b**. As shown in Figure 9 for **5′** and **6′**, the computed LUMO energy difference (−3.0 eV for **5′** vs −1.5 eV for **6′**) is greater than that of the HOMO (−5.2 eV for **5′** to −4.6 eV for **6′**). Hence, the band gap increases from 2.3 eV for **5′** to 3.1 eV in **6′**. The experimental optical band gaps, obtained from the intersection of absorption and emission traces of **5a,b** and **6a** (2.1 and 2.6 eV, respectively) agree reasonably well. For comparison, the solution electrochemical HOMO−LUMO gap is 2.16 eV.

Conclusion

In conclusion, we have prepared a redox interconvertible pair of heterocyclic tetracene derivatives, the aromatic **5a,b** and **7** and their dihydro derivatives **6** and **8**. These compounds are potentially useful as active layers in thin-film transistors. The formation of the requisite films for **5**−**8** is challenging and under current investigation. While **5a,b** are persistent, **6a,b** are readily oxidized to **5a,b** in air. The 4n+2 π species, **5a,b** and **7**, have small band gaps and are red-fluorescent. In contrast, their 4n π dihydro derivatives, **6a,b** and **8**, are green-fluorescent and have significantly larger band gaps. The 4n π compounds, **6a,b** and **8**, display significantly reduced aromaticity when compared to **5a,b** and **7**. The paratropicity of the antiaromatic (4n π) dihydropyrazine subunits is *delocalized* throughout the system. Thus, although they are easily oxidized, large 4n π compounds like **6a,b, 6′**, and **8** are not appreciably destabilized relative to their 4n+2 π congeners, **5a,b, 5′**, and **7**.

Acknowledgment. We thank the National Science Foundation (STC Program, DMR-0120968 (S.B., S.R.M.) and Grants CHE 0716718 (P.S., J.W.) and CHE 0548423 (U.B., S.B.M., S.M.B.) for financial support and Dr. J. Anthony and A. Appleton for helpful discussions.

Supporting Information Available: Synthetic details and NMR spectra as well as the CIF files for **5**−**8**. This material is available free of charge via the Internet at http://pubs.acs.org.

JA077614P

(21) Schleyer, P. v. R.; Maerker, C.; Dransfeld, A.; Jiao, H. J.; Hommes, N. J. R. V *J. Am. Chem. Soc.* **1996**, *118*, 6317–6318.
(22) (a) Corminboeuf, C.; Hein, T.; Seifert, G.; Schleyer, P. v. R. *J. Phys. Chem. Chem. Phys.* **2004**, *6*, 273–276. (b) Chen, Z. F.; Wannere, C. S.; Corminboeuf, C.; Puchta, R.; Schleyer, P. v. R. *Chem. Rev.* **2005**, *105*, 3842–3888. (c) Fallah-Bagher-Shaidaei, H.; Wannere, C. S.; Corminboeuf, C.; Puchta, R.; Schleyer, P. v. R. *Org. Lett.* **2006**, *8*, 863–866.
(23) Schleyer, P. v. R.; Manoharan, M.; Wang, Z. X.; Kiran, B.; Jiao, H.; Puchta, R.; Hommes, N. J. R. V. *Org. Lett.* **2001**, *3*, 2465–2468.
(24) (a) Kutzelnigg, W. *Isr. J. Chem.* **1980**, *19*, 193–200. (b) Pipek, J.; Mezey, P. G. *J. Chem. Phys.* **1989**, *90*, 4916–4926. (c) Malkin, V. G.; Malkina, O. L.; Casida, M. E.; Salahub, D. R. *J. Am. Chem. Soc.* **1994**, *116*, 5898–5908.
(25) (a) Corminboeuf, C.; Heine, T.; Weber, J. *Org. Lett.* **2003**, *5*, 1127–1130. (b) Moran, D.; Manoharan, M.; Heine, T.; Schleyer, P. v. R. *Org. Lett.* **2003**, *5*, 23–26. (c) Heine, T.; Schleyer, P. v. R.; Corminboeuf, C.; Seifert, G.; Reviakine, R.; Weber, J. *J. Phys. Chem. A* **2003**, *107*, 6470–6475.
(26) Schleyer, P. v. R.; Manoharan, M.; Jiao, H.; Stahl, F. *Org. Lett.* **2001**, *3*, 3643–3646.